Journal of the Association of Arab Universities for Basic and Applied Sciences (2010) 9, 6–11

University of Bahrain
Journal of the Association of Arab Universities for Basic and Applied Sciences
www.elsevier.com/locate/jaaubas
www.sciencedirect.com

ORIGINAL ARTICLE

Preliminarily test of physically based models to estimate clear sky emissivity in Tabouk, Saudi Arabia

A.H. Maghrabi [a,*], Z.A. Al-Mostafa [b], M.N. Kordi [c], R.W. Clay [d]

[a] *King Abdulaziz City for Science and Technology, National Center for Mathematics and Physics, P.O. Box 6086, Riyadh 11442, Saudi Arabia*
[b] *King Abdulaziz City for Science and Technology, National Astronomy Center, P.O. Box 6086, Riyadh 11442, Saudi Arabia*
[c] *King Abdulaziz City for Science and Technology, Petroleum and Gas Institute, P.O. Box 6086, Riyadh 11442, Saudi Arabia*
[d] *School of Chemistry and Physics, University of Adelaide, South Australia 5005, Australia*

Available online 14 December 2010

KEYWORDS
Air mass;
Air temperature;
Emissivity;
Solar radiation;
Vapour pressure

Abstract Analysis of the performance of physically based models was done using infrared sky temperature observations taken in Tabouk City, North-West Saudi Arabia, during winter 2005. The models used here are the Brutsaert model and the Prata model. Initially, the original coefficients are used, and then, the coefficients are adjusted according to the observed models' response to the differences between the actual atmospheric vertical structure and the average standard conditions. The produced resulting corrected estimation has reduced the RMSE and MBE values, as compared to those obtained originally. The RMSE and MBE have been reduced from 10.5 and −10 to 3.8 and −1.6, respectively, as the coefficients for the Brutsaert model were adjusted. Similarly, for the Prata model, the RMSE and MBE in the sky temperature values have been reduced from 7.7 °C and −7.2 °C to 2.9 °C and −1.0 °C, respectively.

1. Introduction

Several atmospheric radiation models have been developed for evaluating the atmospheric emittance. Most of these models have been developed by the statistical fitting of experimental data that use screen-level parameters and have local empirical coefficients. Alternatively, there are simple formulae, based on the solution of the radiative transfer equation for the atmosphere, which include coefficients, depending on the vertical distribution, which employ the standard temperature lapse rate and vapour density scale height.

Infrared (IR) atmospheric radiation (wavelength 4.0–100 μm) is a key term in the surface energy budget and is vitally important for climatological and meteorological studies and in applications, such as solar energy, design of radiant cooling systems, and agricultural meteorology. IR radiation may refer to gaseous absorption and emission of the radiation in the atmosphere by green house gases (mainly water vapour, carbon dioxide ozone and to lesser extent some trace gases such as, methane, nitrous oxides). This radiation depends mainly on the distribution and proportion of water vapour,

* Corresponding author.
E-mail addresses: amghrabi@kacst.eud.sa (A.H. Maghrabi), zalmostafa@kacst.eud.sa (Z.A. Al-Mostafa).

Peer review under responsibility of University of Bahrain.
doi:10.1016/j.jaubas.2010.12.003

Production and hosting by Elsevier

carbon dioxide, and ozone in the atmosphere. The proportion of carbon dioxide remains essentially constant over long time scales and ozone is concentrated at higher altitudes, but the proportion of water vapour can change considerably at ground level.

IR atmospheric radiation can be determined by direct measurement using a pyrgeometer, which is relatively expensive or estimated using empirical method.

Several empirical formulae have been developed for both models to calculate IR radiation for clear skies using various parameters. These models were based on the statistical fit between this radiation and the screening-level parameters, such as air temperature and/or vapour pressure (Brunt, 1932; Swinbank, 1963; Clark and Allen, 1978; Idso, 1981; Andreas and Ackley, 1982; Dilley and O'Brien, 1998; Perez-Garcıa, 2004). Because of their empirical nature the physical insight of these models is low and their validity depends on the sufficiency of the used surface data.

Alternatively, some simple semi-empirical models have been obtained by integration of radiative transfer equation and used for simplification hypotheses that allow an approximate for analytical solution in terms of screening-level variables (Brutsaert, 1975; Prata, 1996).

Both these developed empirical and semi-empirical models are suitable for clear-sky conditions where an additional term in clear-sky models is needed to account for clouds to obtain IR radiation for all sky conditions. This corrective term is often the fractional cloud cover (Jacobs, 1978).

If we only consider the physically based models, despite only surface data are used as input variable, these models contain coefficients depending on the vertical structure of the atmosphere that are considered constants after introducing standard values of these parameters describing temperature and water vapour density distributions.

In this study, we present an analysis of the performance of the more relevant of these physically based models using infrared sky temperature observations taken in Tabouk City (Lat: 28°.38 N, Long: 36°.61 E, Elevation: 768 m above sea level), North-West of Saudi Arabia, during winter 2005. Further, locally, we calibrated these models to optimise their performance for estimating night-time clear-sky temperatures in Tabouk.

2. Models

Brutsaert (Brutsaert, 1975) derived his model from the solution of Schwarzschild's radiative transfer equation by employing a few simplifying assumptions to allow an analytical treatment. The effective sky emissivity for clear skies according Brutsaert has the following form:

$$\epsilon_{sky}(T, eo) = c \times \left(\frac{eo}{T}\right)^{m} \tag{1}$$

with

$$c = mA\left(\frac{0.662}{k_2 R}\right) B\left(\frac{k_1}{k_2}, m\right) \tag{2}$$

Where R is the gas constant for dry air, B is the complete Beta function, $k_1 = k_2 + (4\gamma/T)$ and $k_2 = k_v + k_p/2$, and γ is lapse rate of temperature. For typical U.S. standard atmosphere, $k_v = 4.4 \times 10^{-4}\ \mathrm{m}^{-1}$, $k_p = 1.3 \times 10^{-4}\ \mathrm{m}^{-1}$, $\gamma = 0.0065\ \mathrm{K\ m}^{-1}$, and $T = 288.15$ K, in addition to the fitted values of $m = 1/7$ and $A = 0.75$ and by using the above-mentioned typical value of the constants yields $c = 1.24$.

Finally, Brutsaert final form for the clear sky emissivity is:

$$\epsilon_{sky}(T, eo) = 1.24 \times \left(\frac{eo}{T}\right)^{\frac{1}{7}} \tag{3}$$

In Brutsaert's formulation, in the case of a very dry atmosphere, the sky emissivity would approach toward zero, that eliminated the possible contribution from atmospheric components different to the water vapour as the aerosols or as even, the CO_2 or the O_3.

Prata (1996) has proposed a model that attempts to solve the outlined problem by a new adjustment of the slab emissivity data. This model is expressed in the following way:

$$\epsilon_{sky}(IWV) = 1 - (1 - IWV)e^{-(C + D \times IWV)^{\frac{1}{2}}} \tag{4}$$

where IWV is the integrated in cm extrapolated from the screening-level temperature and vapour pressure, and given as

$$IWV = \alpha\left(\frac{e_0}{T}\right) \tag{5}$$

The constants C, D, and α take the values 1.2, 3 and 46.5 in the Prata's original model, respectively.

3. Data and methods

3.1. Instruments and data collection

The observational data set used in this study consists of sky temperature measurements from the IR detector, surface meteorological data, and upper air temperature and humidity profiles from radiosondes. The observations were taken during the winter season between January and March 2005.

The IR sky temperature (T_{sky}) was measured using a single-pixel, broadband IR detector designed by our group where the construction of this instrument, its calibration, and all related technical issues have been described elsewhere (Clay et al., 1998; Riordan et al., 2005; Maghrabi, 2007; Maghrabi et al., 2009). The basic detector is a Heimann TPS 534 thermopile. For the present study the angular field of view was set to 90° (full width at half-maximum) using a Fresnel lens. The spectral response for the assembly of the thermopile and the lens extends from 5.5 μm to >20 μm. The experimental error for T_{sky} measurements is approximately 2 °C (Maghrabi, 2007). In addition, theoretical simulations using MODTRAN software (Berk et al., 1989) revealed good agreement with measured sky temperatures, with a root mean square error (RMSE) in the temperature of approximately 1.5.

The data acquisition system was XR5-8-A-SE data logger manufactured by Pace Scientific. In addition to the temperature sensor within the detector, the loggers have internal sensors to measure the humidity and the surface temperature. The data were logged in 10 min intervals. The accuracy of the logger's sensor measurements is ±2% humidity and ±15 °C at a temperature of 25 °C.

Standard meteorological data for air temperature T, dew-point temperature T_{dp}, air pressure P, relative humidity RH, and cloud formation were obtained from Tabouk Airport records provided by the Presidency of Metrological and Environment (PME). Vapour pressure e_0 and specific humidity q were calculated from T_{dp}, T and P according to the procedures outlined elsewhere (Maghrabi, 2007).

Hourly data were used in the analysis to avoid clustering of data over a short range of conditions. No major differences were found between logger/calculated records and those measured by the PME. For example, the difference between the calculated T_{dp} and the measured values was always below 2 °C.

At the site, the assembly of the IR detector and the logger was installed in a stand especially designed by KACST for the purpose of this study – Fig. 1.

During the period of operation the detector showed a linear and stable performance. No significant changes in the detector and the logger system sensitivity have been identified, even after continuous exposure to extreme weather conditions. Regular hardware checks were carried out for the system. Apart from changing the batteries no major breakdown or any faults were found.

3.2. Clear sky selections

Clear sky data were selected using the methods described earlier (Maghrabi, 2007; Maghrabi and Clay, 2008; Maghrabi et al., 2009). These procedures used two sources of information, cloud data provided by PME and data from the IR detector. For example, in selecting clear sky periods during a specific day the following was made:

1. The visually observed total cloud cover reported by PME at the site has to be less than one octa. Although these observations are kept in PME database, some periods during specific days were not available. This method was used as an initial tool to identify the clear sky times.
2. Plotting sky temperature versus time for the desired day when the cloud cover less than one octa was then performed. Taking in account that cold temperatures represent clear sky and warm temperatures indicate cloudy periods. This is because clouds enhance the IR emission in the region between 8 and 14 μm which is covered by the IR detector. Selecting clear sky times using this method is illustrated in Fig. 2.

We had collected data at night for this study to avoid any possible bias due to heating and subsequent re-radiation from the IR transmitting optics of the detector. Clear-sky data were not used for time intervals of < 30 min to avoid spurious data clustering in a limited number of observation periods. A summary of the main parameters for measurements in this study is given in Table 1.

Figure 1 Shows the setup of the monitor/logger system at the field site.

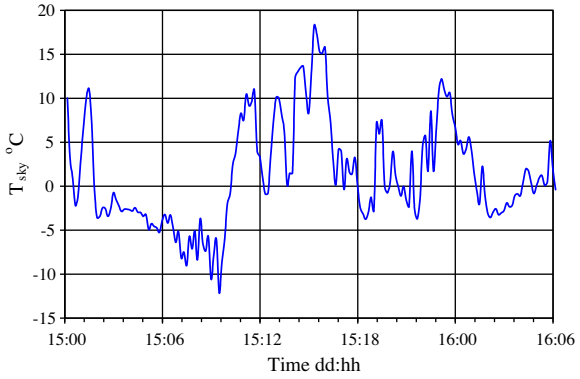

Figure 2 Example shows a plot for two nights with different sky conditions between 15.12.2005 midnight to 16.12.2005 morning. The night starts with some clouds (positive T_{sky}) and then the sky becomes clear (negative T_{sky}) between 0300 and 0900. The sky conditions then varied between clear and cloudy until the next morning.

3.3. Methodology

The atmospheric radiation can be expressed in two ways:

(a) The sky is assumed to behave like blackbody, with emissivity of 1, where in this case the atmospheric radiation is given by:

$$R_{sky} = \sigma \times T_{sky}^4 \tag{6}$$

(b) The sky is assumed to be a grey body with an apparent emissivity, ε_{sky}, defined as:

$$R_{sky} = \sigma \times \epsilon_{sky}^4 \tag{7}$$

In both equations R_{sky} is the measured atmospheric radiation, T and T_{sky} are the air temperature and the sky temperature, respectively, (both in K) and σ is Stefan–Boltzman constant, ε_{sky} is the sky emissivity.

Atmospheric radiation/emittance was calculated using the Brutsaert and Prata models (Eqs. (3) and (4)), and then converted to sky temperatures using Eqs. (6) and (7). For each parameterisation, predicted values of the sky temperature were compared to the measured values via two statistical parameters namely, the root mean square error (RMSE) and the mean bias error (MBE):

Table 1 Overall statistics for clear-sky night-time values of relative humidity RH the dew-point temperature T_{dp}, vapour pressure e_0, air temperature T and IR sky temperature T_{sky} for the considered period. All temperatures are in °C.

Variable	Minimum	Maximum	Mean	Std. Dev.
RH%	17	93	50.47	15.88
T_{dp}	−11.54	10.46	−1.22	3.88
$e_0$mb	2.53	12.67	5.79	1.74
T	−0.36	22.63	7.91	4.47
T_{sky}	3.89	−10.66	−5.27	3.38

Table 2 Performance of the two considered LW clear-sky models in their original forms compared to sky temperatures measured for Tabouk. MBE is the mean bias error, RMSE is the root mean square error, *a* is the slope, *b* is the intercept of the regression line, *r* is the correlation coefficient.

	Minimum	Maximum	Mean	MBE	RMSE	*a*	*b*	*r*
Brutsaert	11.20	−16.48	−5.46	−0.19	3.48	1.40	1.92	0.82
Prata	10.14	−14.84	−5.39	−0.121	2.68	1.27	1.32	0.86

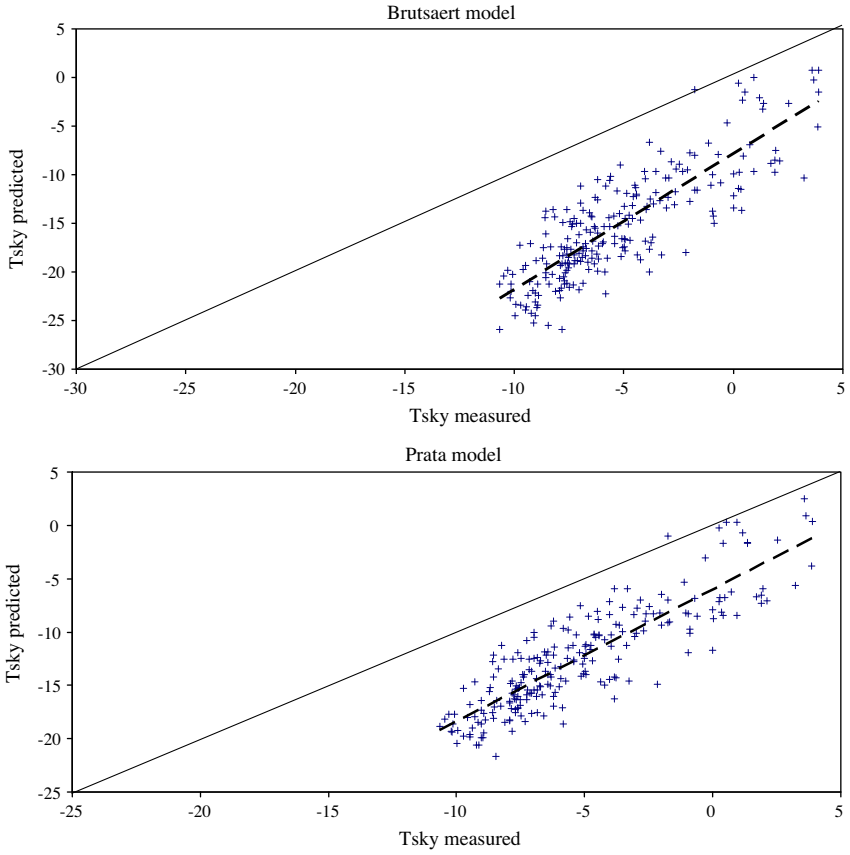

Figure 3 Comparison of measured and predicted sky temperatures for the Brutsaert (top) and Prata (bottom) models in their original forms. The dashed line is the regression fit between T_{sky} predicted and measured. The solid line is the 1:1 line for reference.

$$\mathrm{RMSE} = \left[\frac{1}{n}\sum_{i=1}^{n}(y_i - x_i)^2\right]^{0.5} \tag{8}$$

and

$$\mathrm{MBE} = \frac{1}{n}\sum_{i=1}^{n}(y_i - x_i) \tag{9}$$

Simple linear regression of the form $y = ax + b$ of the relationship between measured and predicted values was performed to evaluate the proximity between the calculated and observed temperatures.

For each model we calculated the slope *a* intercept *b*, and correlation coefficient *r*. A good predictor should have a small MBE and RMSE, *r* close to 1, an intercept close to zero, and a best-fit slope close to 1.

4. Results and discussion

The calculated sky temperatures by the two models with their original coefficients and the comparison against the measured data are presented in Table 2 and Fig. 3. At warmer sky temperatures the calculated sky temperatures by Brutsaert and Prata models do not differ much from the measured values (this being 2.4 °C for the former and 0.72 °C for the latter). At cold sky temperatures the difference between the Brutsaert and the measured values is ~25 °C and that between Prata and the measured values is ~22 °C. This means that both models are predicting reasonably good at warm sky temperatures and failed to do so at cold temperatures.

The MBE and RMSE for both models showed that both models are overestimating the measured sky temperatures ~10 °C and ~7 °C for Brutsaert and Prata, respectively. The slope and the intercepts values showed larger deviation from

Table 3 Performance of the two considered Atmospheric clear-sky models in their calibrated forms compared to sky temperatures measured for Tabouk.

	Minimum	Maximum	Mean	MBE	RMSE	*a*	*B*	*r*
Brutsaert	0.77	−25.90	−15.28	−10.01	10.54	1.36	−7.88	0.85
Prata	2.48	−21.63	−12.53	−7.26	7.70	1.23	−6.01	0.85

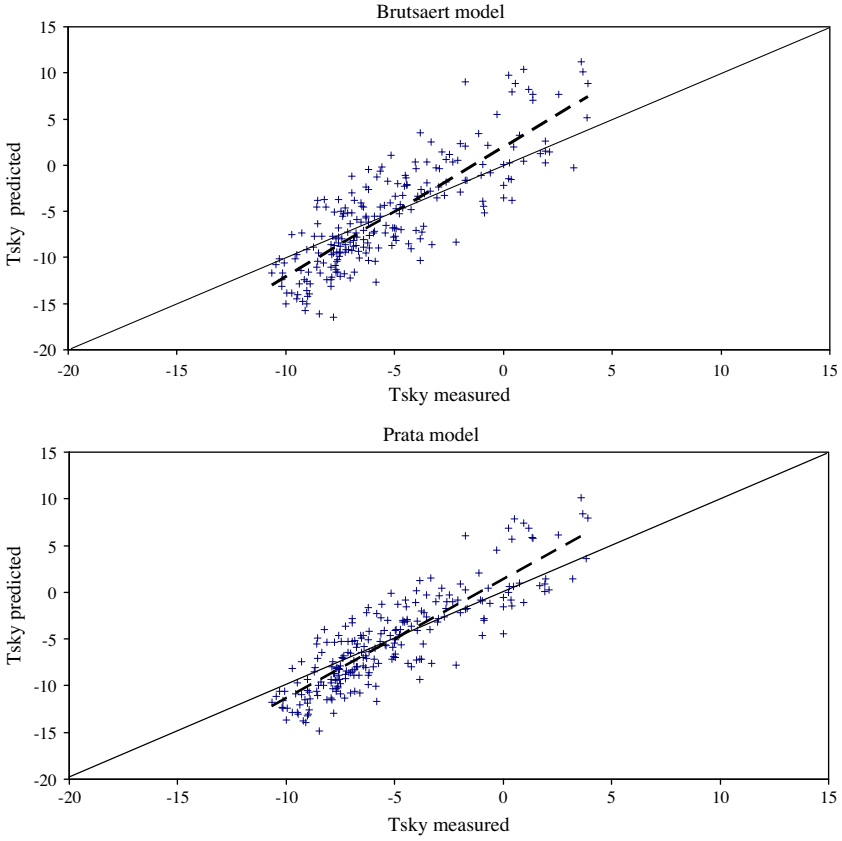

Figure 4 Comparison of measured and predicted sky temperatures for the Brutsaert (top) and Prata (bottom) models in their newly calibrated forms. The dashed line is the regression fit between T_{sky} predicted and measured. The solid line is the 1:1 line for reference.

the measured sky temperatures as it is evident from Fig. 3. However, the general performance of Prata model showed better statistics than the Brutsaert model.

To optimize the performances of these two models we locally calibrated them and adjusted their coefficients to suit the atmospheric conditions found in Tabouk city. The least square fit for the experimental data yield the following functional form for the Brutsaert and Prata models, respectively as:

$$\epsilon_{sky} = 1.44\left(\frac{e_0}{T}\right)^{1/7} \tag{10}$$

$$\epsilon_{sky} = 1 - \left(1 + 40 \times \frac{e_0}{T}\right) e^{-\left(1.55+4.8\times 40\times \frac{e_0}{T}\right)^2} \tag{11}$$

The values of the coefficients are rather higher than those of the original ones and they can reflect the extreme atmospheric conditions found in Tabouk in this time of the year. The performance of the new calibrated models is reported in Table 3. The new equations showed MBE values less than half a degree with a RMSE values of 3.48 and 2.68 for Brutsaert and Prata models, respectively. Comparing the MBE, RMSE and the intercept values for the calibrated models with those of the original forms shows that the calibrated models are able to produce better performances.

However, the slopes of the new calibrated models are deviated from the optimum value of 1. Fig. 4 shows the calculated sky temperature by the calibrated models against the measured temperatures. The solid line is the 1:1, which represents the ideal match between measured and estimated temperatures, and the dashed line is the regression line.

Most of the data lies in the 1:1 line or in the vicinity of it, which may show the suitability of the new calibrated models in calculating the sky temperatures in Tabouk during winter times. Some deviations at very high and very low sky temperatures are evident. This may be due to some extreme atmospheric conditions that occurred during winter times such as strong temperature inversions or the effect of the cold fronts as well as the effect of other parameters such as the wind speed and aerosol particles which have not been accounted for by

these two models. This matter will be investigated in future study.

5. Conclusion

The aim of this study to evaluate the performance of two physically based models in computing IR sky temperatures during winter times in Tabouk city was evaluated. These selected models were based on a simplified solution of the radiation transfer equation. IR sky temperatures calculated by these models were compared to hourly averaged clear-sky night-time measurements in Tabouk during the winter times 2005. It was found that the models in their original form do not produce comparative results with the measured data. These two models were further calibrated using the least square fit. These calibrations, generally, performed well in predicting most of the measured data. However, larger deviations were found and this may be due to the effect of the other parameters that were not considered in the calibrations such as the actual temperature and density profiles. This subject will be further investigated in another study.

References

Andreas, E.L., Ackley, S.F., 1982. On the differences in ablation seasons of Arctic and Antarctic sea ice. J. Atmos. Sci. 39, 440–447.

Berk, A., Bernstein, L.S., Robertson, D.C., 1989. MODTRAN: a moderate resolution model for LOWTRAN7. Report GL-TR-89-0122, Geophysics Directorate, Phillips Laboratory, Bedford, MA.

Brunt, D., 1932. Notes on radiation in the atmosphere. Q. J. R. Meteorol. Soc. 58, 309–420.

Brutsaert, W., 1975. On derivable formula for long-wave radiation from clear skies. Water Resour. Res. 11, 742–744.

Clark, G., Allen, C.P, 1978. The estimation of atmospheric radiation for clear and cloudy skies. In: Prowler, Don, Duncan, Ian (Eds.), Proc. 2nd Nat. Passive Solar Conf., vol. 2. University of Pennsylvania, Philadelphia (March. 1978), p. 676.

Clay, R.W., Wild, N.R., Bird, D.J., Dawson, B.R., Johnston, M., Patrick, R., Sewell, A., 1998. A cloud monitoring system for remote sites. Pub. Astron. Soc. Aust. 15, 332–335.

Dilley, A.C., O'Brien, D.M., 1998. Estimating downward clear sky long-wave irradiance at the surface from screen temperature and perceptible water. Q. J. R. Meteorol. Soc. 124, 1391–1401.

Idso, S.B., 1981. A set of equations for full spectrum and 8 to 14 μm and 10.5 to 12.5 μm thermal radiation from cloudless skies. Water Resour. Res. 17, 295–304.

Jacobs, J.D., 1978. Radiation climate of Broughton Island. Energy budget studies in relation to fast-ice breakup processes in Davis Strait. Occas. Pap., vol. 26. Inst. of Arctic and Alp Res., University of Colorado, Boulder, United States, pp. 105–120.

Maghrabi, A.H., 2007. Ground Based Measurements of IR Atmospheric Radiation from Clear and Cloudy Skies, Ph.D. Thesis. University of Adelaide, Adelaide, Australia.

Maghrabi, A.H., Clay, R., Wild, N., Dawson, B., 2009. Design and development of a simple infrared monitor for cloud detection. Energy Convers. Manage. 50 (11), 2732–2737.

Maghrabi, A.H., Clay, R.W., 2008. Results from a Simple Infrared Cloud Detector, Accepted as a Peer Reviewed Paper in the International Solar Energy Society – Asia Pacific Conf. 25–28 Nov 2008 (WC0160).

Perez-Garcıa, M., 2004. Simplified modeling of the nocturnal clear sky atmospheric radiation for environmental applications. Ecol. Model. 180, 395–406.

Prata, A.J., 1996. A new long-wave formula for estimating downward clear-sky radiation at the surface. Q. J. R. Meteorol. Soc. 122, 1127–1151.

Riordan, D., Clay, R., Maghrabi, A., Dawson, B., Wild, N., 2005. Cloud base temperature measurements using a simple long wave infrared cloud detection system. J. Geophys. Res. 110, D03207. doi:10.1029/2004JD005390.

Swinbank, W.C., 1963. Long-wave radiation from clear skies. Q. J. R. Meteorol. Soc. 89, 339–348.